FRACTOGRAFIC STUDY OF CLEAVAGE CRACK ARREST

M. Hajjaj [1,2], C. Berdin [2], P. Bompard [2] and S. Bugat [1]

[1] Electricité de France, R&D Division, Département MMC, Les Renardières, 77818 Moret-sur-Loing cedex France

[2] Laboratoire de Mécanique Sols, Structures et Matériaux, Grande Voie des Vignes, 92295 Châtenay-Malabry France

ABSTRACT

The aim of the study is to understand micromechanisms of cleavage crack arrest under thermal shock on A533 Cl.B type steel. Thermal shock experiments on notched disc were performed and crack arrest was obtained for arrest temperatures ranging from –120°C up to –55°C. Fractographic observations were performed using scanning electron microscope (SEM). The use of the Mex V4.0 software linked to the Philips XL-30 SEM allowed to obtain 3-D information on fracture surface.

Characteristics patterns were observed, some confirmed classical results, others were not already reported. The results obtained showed that the mode of fracture at crack arrest is cleavage. The arrest front is very curved. The analysis of an area near the crack arrest front showed the presence of several ligaments broken by shearing that could be the dominant energy-absorbing mechanism with crack branching. The study of the edge of the crack arrest front showed the presence of a flat area that could be ductile tearing crushed. Finally a pre-crack arrest zone starting at the edges of the crack arrest front was evidenced, which delimits two different roughness surfaces.

1 INTRODUCTION

The use of crack arrest concept in structural integrity can be taken as a supplementary level of assessment, which completes the initial assessment usually based on initiation (Burdekin [1]). For reactor pressure vessels (RPV) of pressurized water reactors (PWR) submitted to pressurized thermal shocks (PTS), it is important to know if a crack could stop before it goes through an unstable proportion of the entire vessel thickness (usually ¾). It is therefore important to understand the micromechanisms of propagation and crack arrest and to determine characteristics features leading to energy dissipation.

This study is focused on micromechanisms of crack arrest phenomenon using a thermal shock experiment performed on a notched disk taken from a A533 Cl.B type steel. This test is supposed to be representative of a RPV submitted to a PTS, although its dimensions are much smaller. The specimen consists in a ring of internal diameter 50mm, external diameter 150mm, and a thickness of 20mm. A straight defect is obtained by fatigue pre-cracking on the outer surface of the disk. The disk is first plunged into liquid nitrogen (-196°C), then raised up to an electromagnetic inductor, placed on its center. The inner surface of the disk is elevated at about 600°C, thus inducing high tensile stresses on the cold outer part of the ring and therefore allowing the initiation of a cleavage crack. Since crack propagates towards a more ductile material due to temperature rise, crack arrest can be obtained.

Four thermal shock experiments were performed. Thermo-mechanical analysis were reported elsewhere (Hajjaj et al. [3]). Post-experiment fractographic observations revealed microstructural mechanisms of crack propagation and arrest. The Mex V4.0 software was linked to the Philips XL-30 SEM to analyse the roughness of the surface specimen using 3D images.

2 MATERIAL AND EXPERIMENTAL PROCEDURES

2.1 Material

A French steel 18MND5 (equivalent to the American ASTM Standard A533 Cl.3) extracted from a heavy section rolled sheet was studied. Its chemical composition is given in Table 1. The material was submitted to heat treatment including one austenitization (900°C during 6h), followed by water quenching, tempering and final stress relief treatment at 615°C during 16h. The RT_{NDT} of the material is -40°C. The resulting microstructure is tempered bainite (Fig. 1). Bainitic packet size is about 5-10 μm, with prior austenitic grain about 20-30μm.

C	Mn	Ni	Mo	P	S	Si	Cr
0.18	1.51	0.66	0.50	0.006	0.003	0.22	0.18

Table 1: Chemical composition of 18MND5 steel (weight %).

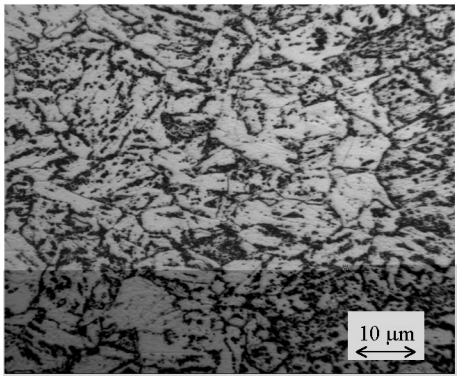

Figure 1: Microstructure of 18MND5 steel (optical microscopy, nital etching).

2.2 Thermal shock experiment

This test was developed by Ecole des mines de Paris (Genty [2]). The specimen consists in a ring with 50mm in inner diameter, 150mm in outer diameter (Figure 2) and 20mm in thickness. A straight defect located on the outer surface was obtained by a notch followed by a fatigue pre-crack. Two different defect sizes (a/w = 0.30 and 0.46, see Figure 2) were studied.

The disk is first cooled up to –196 °C thanks to liquid nitrogen in order to simulate the end-of-life embrittlement of the material due to irradiation. The disk is then raised up and the temperature of the inner surface of the disk is heated thanks to a magnetic inductor. The resulting thermal field within the specimen produces high tensile stress on the cold outer part of the ring, inducing the opening of the crack. When the initiation fracture toughness (K_{IC}) is reached, a brittle crack extends towards a tougher material that induces a crack arrest event after a few centimetres of propagation. More information about thermal shock test are available elsewhere (Hajjaj et al. [3]). Crack velocity was measured about 600m.s^{-1}.

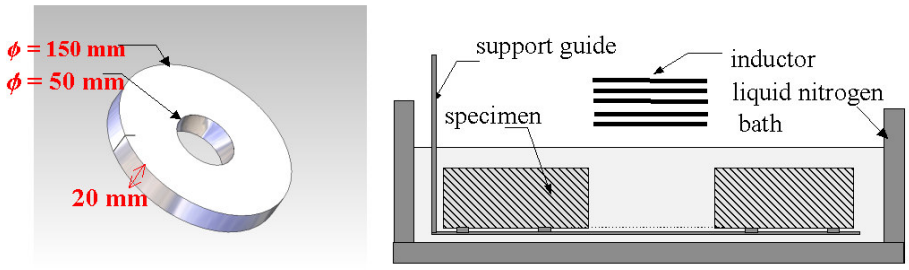

Figure 2: Specimen geometry and test principle.

2.3 Fratographic observations

Fractographic observations were performed on the four specimens, using a Philips XL-30 scanning electron microscope (SEM) operating at 20 KeV. The working distance was about 10mm. After thermal shock test, crack arrest front was identified by heat tinting or by fatigue cracking; the specimens were finally fractured at cold temperature (-196°C). However heat tinting did not allow to identify the crack arrest front on SEM images even though it was visible to the naked eye, and this procedure was then avoided. To eliminate corrosion marks, specimens were treated with a mixture of HCl 10 % and phenyl thiourea.

According to the macrography (Figure 3), one can see that the arrest front is very curved. Indeed the difference between the maximum crack length and the crack length at the edges is about 5mm. Table 2 summarized crack jump lengths and arrest temperature, *i.e.* temperature at the arrest location, and the arrest fracture toughness computed from elastic-static analyses (Hajjaj et al. [3]). For each specimens, three areas were particularly studied. Location of these areas are identified in figure 3. The first area, related to the crack arrest front, is shown in figure 4. According to this figure, the fracture mode at crack arrest is cleavage.

Test	a_0 (mm)	a_f (mm)	T arrest (°C)	K_{Ia} (MPa.m$^{1/2}$)
T22	notched	39.0	-56.0	138.0
D02-1	16.2	40.4	-104.5	98.7
D02-2	15.8	39.8	-91.0	115.6
D025-10	23.9	42.6	-124.0	62.6

Table 2: Initial and final crack length (maximum value), arrest temperature and static arrest toughness

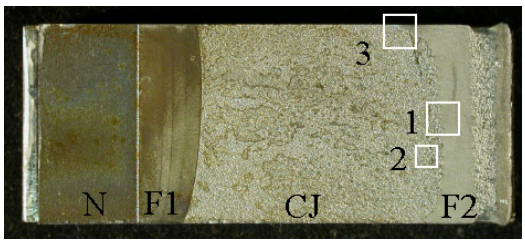

Figure 3: Specimen macrography ; N, the notch, F1, the fatigue pre-crack, CJ the crack jump due to thermal load, F2, the post-fatigue; boxes 1, 2 and 3 locate the figures 4, 5 and 6.

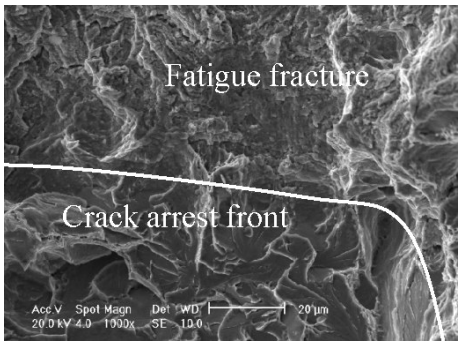

Figure 4: Crack arrest front: box 1 in figure 3.

In order to highlight the difference in relief observed between the beginning and the end of the propagation, we used the Mex V4.0 software (made by the company Alicona) linked to the Philips XL-30 SEM. This software allowed us to obtain a 3D image using two 2D images tilted by an angle of 5 or 10 degrees. This technique was used to observe the areas 2 and 3. The area 2, related to the region near the crack arrest front, is shown in figure 5. In this region, in addition to cleavage facets, one can highlight the presence of important sheared ligaments without dimples. The graphics of the figure 5 give the relief along the white arrow in the image and show that shearing can reach a value of 125 µm which corresponds to two or three prior autenitic grains.

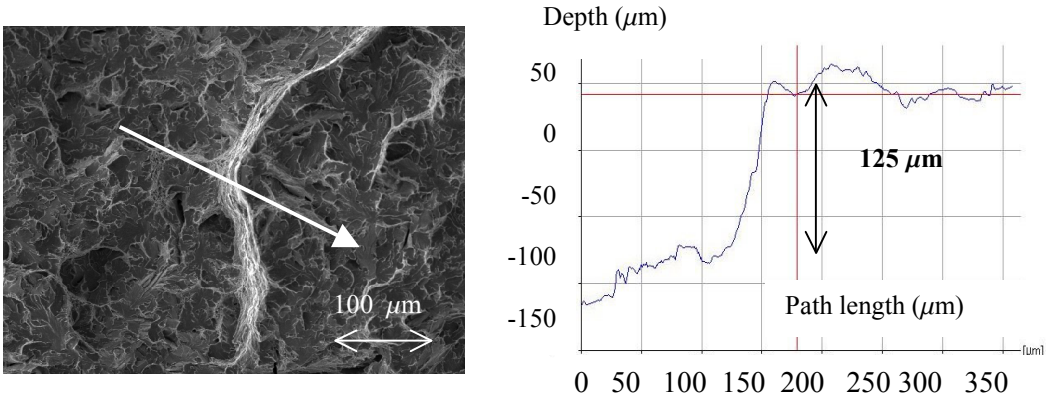

Figure 5: Sheared zone (box 2 in figure 3).

The third area studied is the arrested crack front at the specimen sides (Figure 6) . The particularity of this area is the presence of a flat zone. The graphics corresponding to the image confirm this observation and shows that the thickness of this flat zone is about 150 µm. Indeed, this flat zone is observed for all the specimens opened by fatigue, but also for specimens opened at cold temperature just after heat tinting. Moreover, this zone is not present in all the crack arrest front but is limited to the sides of the specimen.

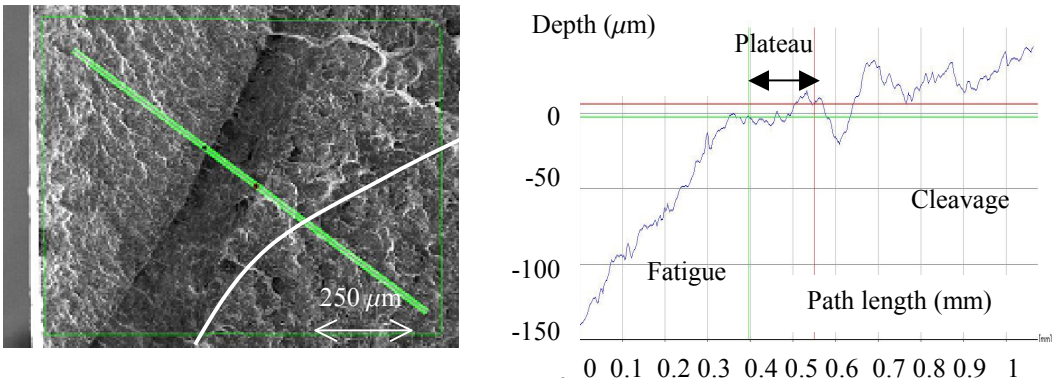

Figure 6: Crack edge (box 3 in figure 3) : dark line is the path along which the height is measured, white line marks the boundary of the "pre-arrest" zone where roughness is larger.

3 DISCUSSION

Thermal schock specimens all fractured showing the same features, independently on the initial crack length or arrest temperature. At the center of the specimen, the crack arrested in "pure" cleavage mode. Very scarce ductile ligaments showing dimples were observed as reported by several authors (Hoaglang et al. [4], Genty [2]). Far from crack arrest, cleavage facets even perpendicular to the macro-crack plane can be noticed, indicating that almost any cleavage cristallographic plane ahead of the propagating crack tip can become critical as the crack front propagates at very high speed. The cleavage criterion seems to be easily satisfied.

Neverthless, crack arrest seems to occur first on both sides of the specimen leaving a flat zone. Linked to this zone and just before the center crack arrest front, a band of about 1mm can be noticed, where the roughness of the cleavage fracture surface is more pronounced (Fig. 6): perpendicular highly sheared faces linking cleavage planes in large bainitic lath colonies are present (see fig. 5). They could correspond to adiabatic shearing since local strain rates must be very high. This probably indicates that, after crack arrest on both sides, the cleavage criterion is then more difficult to reach along the inner crack front and that the crack must sharply deflect to follow the cleavage critical path, as already reported (Rosenfield et al. [5]).

However, although there are signs of dissipative phenomenon, the crack stopped in cleavage mode at the center of the specimen. This is partly in relation with the low value of the crack arrest temperature ($\approx$ -100°C). It is also worth to notice that no isolated cleavage facet was found ahead of the crack tip in the post fatigue fracture surface, and that the arrested crack front is rather regular, even at microscale. So, cleavage propagation and arrest, in the conditions of this thermal schock test, is probably such that a collective behaviour of grains has to be invoked with a binary response: all the grains cleave or no grain cleave at all. So, contrary to cleavage initiation conditions, very strong corrrelation between grains is suspected. Theories proposed by Majundar et al. [5] or Rafiee et al. [6] do not apply: it seeems that no micro-crack nucleation can shield the loading of the macro-crack tip, and the stress intensity factor can be assessed using a macro-crack length which can be easily defined. More insights in this collective behaviour can be found in theory as developped by Tanguy et al. [7].

The situation on the specimen sides is different. The arrested crack front shows a pronounced curvature which is classically observed in cleavage crack arrest experiment (Kobayashi et al. [8]). A flat fracture zone is observed where no classical features (dimples or cleavage facets) can be detected. This zone seems to be crushed. The flat zone observed can be ductile tearing crushed back due to dynamic closing of the crack lips: oscillations can appear at crack arrest which can close the crack. It is also possible that crack closing which occurs after thermal unloading takes place mainly on streched crack sides. Anyway, crack arrest occurs probably first at the specimen sides because stress or temperature gradient due to the free surfaces lead to surface conditions such that cleavage criterion is no more satisfied. After this surface arrest, inner cleavage crack shows more prononced relief and large ductile tearing linking fractured bainitic lath colonies, and then stops in "pure" cleavage mode. Which precise influence has the crack arrest at the free surfaces on the crack arrest at the specimen center, remains an open question: it can be a combination of stress unloading, crack speed decrease, and increasing temperature.

CONCLUDING REMARKS

Cleavage crack arrest experiments were performed on notched thermal shock disc. Crack arrests were obtained at low temperature. Fracture surfaces reveal that propagating cracks arrested in cleavage mode with scarce ductile ligaments, except on the sides of the specimen where a crushed zone probably fractured in ductile mode was observed at crack front.
No micro-crack ahead of the crack tip was detected and the regular shape of the arrested crack front invokes a collective behaviour of the grains at crack arrest, contrary to cleavage crack initiation.

REFERENCES

[1] Burdekin F.M., Knott J.F., Sumpter J.D.G., Sherry A.H., «TAGSI views on aspects of crack arrest philosophies for pressure vessels with thickness up to 100mm», Pressure Vessels and Piping, 76, 879-883, 1999.
[2] Genty A., « Etude expérimentale et numérique de l'amorçage et de l'arrêt de fissure sous choc thermique, dans un acier faiblement allié (16MND5) », Ph.D. Thesis, Ecole des Mines de Paris, France, 1989.
[3] Hajjaj M., Bugat S., Berdin C., Bompard P., «K_{Ia} crack arrest toughness assessment using thermal shock on notched disks », Proceedings of ASME Pressure Vessels and Piping Conference 2004, Fatigue, Fracture & Damage Analysis, to be published.
[4] Hoagland R.G., Rosenfield A.R., Hahn G.T., «Mechanism of fast fracture and arrest in steels », Met. Trans., Vol. 3, pp. 123-136, 1972.
[5] Rosenfield A.R., Majumdar B.S., «A micromechanical model for cleavage crack reinitiation », Met. Trans., Vol. 18A, pp. 1053-1059, 1987.
[6] Rafiee S., Gross D., Seelig Th., «The influence of micro crack nucleation on dynamic crack growth – a numerical study », Eng. Fract. Mech., vol.71, pp. 849-857, 2004.
[7] Tanguy A., Gounelle M., Roux S., « From individual to collective pinning effect of long range elastic interactions », Phys. Rev. E, vol.58, pp. 1577-1590, 1998.
[8] Kobayashi T., Giovanola J.H., «Crack opening profile observations for dynamic cleavage crack propagation and arrest », J. Mech. Phys. Sol., vol. 37, p759-777, 1989.